

Delayed activation of Bax by DNA damage in embryonic stem cells with knock-in mutations of the Abl nuclear localization signals

M Preyer¹, C-W Shu^{1,2} and JYJ Wang^{*,1}

The non-receptor tyrosine kinase Abl contains nuclear localization (NLS) and nuclear export signals that drive its nucleocytoplasmic shuttling. The nuclear Abl tyrosine kinase is activated by DNA damage through ataxia telangiectasia mutated (ATM). Previous studies have suggested nuclear Abl to have proapoptotic activity. To determine the requirement for Abl nuclear import in DNA damage-induced apoptosis, we took a genetic approach by mutating the three NLS (μ NLS) of *abl1* in mouse embryonic stem (ES) cells through homologous recombination. Exposure of ES cells to genotoxins caused an ATM-dependent nuclear accumulation of Abl but not Abl μ NLS. ES cells expressing Abl μ NLS exhibited delayed Bax activation, reduced cytochrome *c* release and decreased caspase-9 activity in response to DNA damage. These results provide a genetic proof that Abl nuclear entry contributes to DNA damage-induced activation of the intrinsic apoptotic pathway.

Cell Death and Differentiation (2007) 14, 1139–1148. doi:10.1038/sj.cdd.4402119; published online 16 March 2007

The mitochondria-dependent intrinsic apoptotic pathway is one of several death mechanisms activated by DNA damage.¹ Transduction of DNA damage signal to mitochondria requires p53, which stimulates cytochrome *c* release through transcription-dependent and -independent pathways.² Although the critical role of p53 is well established, DNA damage-induced apoptosis also occurs through p53-independent mechanisms.^{3,4} We have been interested in the role of Abl as a p53-independent activator of DNA damage-induced apoptosis.^{3,4} The ubiquitously expressed non-receptor tyrosine kinase Abl contains three nuclear localization signals (NLS), one nuclear export signal and undergoes nucleocytoplasmic shuttling in proliferating cells.⁵ In the cytoplasm, Abl responds to growth factor and adhesion signals to regulate F-actin dynamics.⁶ In the nucleus, Abl kinase activity is cell-cycle regulated through its interaction with the retinoblastoma protein RB.⁷ Nuclear Abl kinase activity is further increased when cells are exposed to DNA damaging agents, including cisplatin and ionizing radiation (IR),^{4,8} but Abl is not activated by UV irradiation.⁹ Experiments with cell lines derived from human colon, breast, liver, and thyroid cancers, and in fibroblasts derived from mouse embryos, have suggested Abl to activate p73, a transcription factor of the p53-family, thus leading to the induction of apoptosis.^{4,10–14} Furthermore, a previous finding showed that nuclear entrapment of oncogenic BCR-ABL can also lead to cell death.¹⁵ Taken together, these results suggest that nuclear Abl has a proapoptotic function.

To determine whether nuclear localization of Abl is required for DNA damage-induced apoptosis, we have taken a genetic approach to inactivate the three NLS of Abl by substitution mutations in mouse embryonic stem (ES) cells. Previous studies have shown mouse ES cells to undergo mitochondria-dependent apoptosis in response to genotoxic stress.^{16–18} We therefore examined DNA damage-induced apoptosis in ES cells expressing Abl or Abl μ NLS. We found that cisplatin and IR, but not UV, induced nuclear accumulation of Abl, and this response was abolished by the NLS mutations. We also found that the apoptotic response of ES cells to genotoxins did not require ongoing transcription or the Abl kinase activity. Nevertheless, the Abl μ NLS ES cells exhibited a delayed apoptotic response providing genetic proof for the requirement of Abl nuclear import in genotoxin-induced apoptosis.

Results

Construction of Abl μ NLS ES cells. Substitution mutations of 11 basic amino acids (Lys and Arg) in the three Abl NLS with Gln has previously been shown to block nuclear import of ectopically expressed Abl.¹⁹ We therefore designed a targeting vector (Supplementary Figure 1) to introduce 15 base changes resulting in 11 substitution mutations of the three NLS in the endogenous *abl1* gene of mouse ES cells (Figure 1a and b). Six G418-resistant clones were identified

¹Division of Hematology-Oncology, Department of Medicine, and Moores-UCSD Cancer Center, University of California, San Diego School of Medicine, La Jolla, CA, USA

*Corresponding author: JYJ Wang, Moores-UCSD Cancer Center, Room 4328, 3855 Health Sciences Drive, La Jolla, CA 92093-0820, USA. Tel: +1 858 534 6253; Fax: +1 858 534 2821; E-mail: jywang@ucsd.edu

²Current address: Department of Life Science and Institute of Biotechnology, National Tsing Hua University, Hsinchu, Taiwan, 30013, ROC.

Keywords: ATM; caspase; cisplatin; embryonic stem cells; leptomycin B; p53

Abbreviations: NLS, Nuclear localization signals; NES, Nuclear export signals; IR, ionizing radiation; ES, embryonic stem cells; LMB, Leptomycin B; ATM, ataxia telangiectasia mutated

Received 09.10.06; revised 16.1.07; accepted 05.2.07; Edited by M Oren; published online 16.3.07

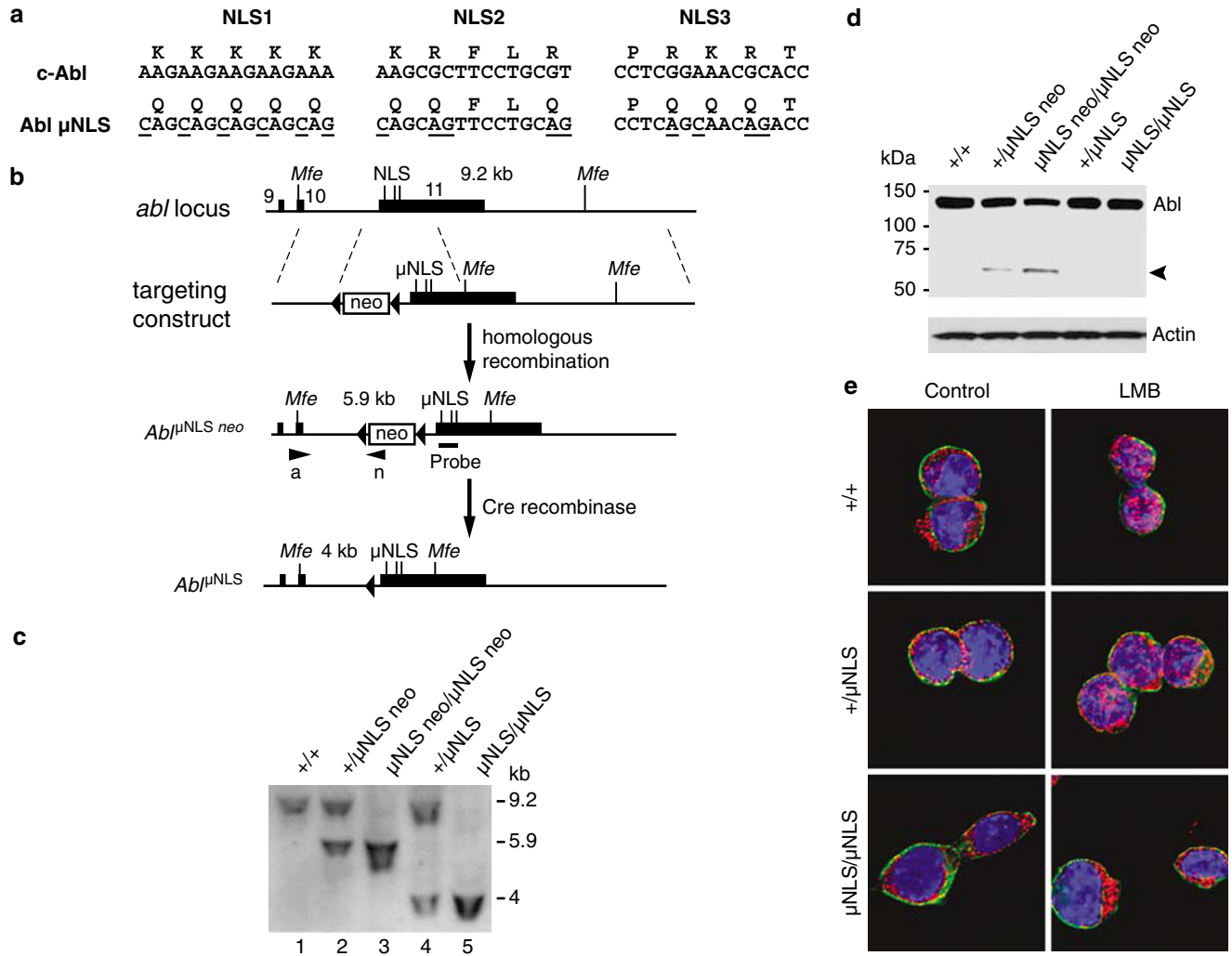


Figure 1 Generation of ES cells expressing exclusively cytoplasmic Abl. (a) Sequences of the three NLS of mouse c-Abl. All lysines (K) and arginines (R) are mutated to glutamine (Q) in Abl μ NLS. The base mutations leading to amino acid changes are underlined. (b) Targeting strategy. The targeting construct contains exon 11 encoding the three NLS. A PGK/Neo cassette flanked by loxP sites (arrowheads) was inserted in intron 10, and an MfeI restriction site was created in the 3' UTR of exon 11. Positions of primers (a and n) and Southern probe used to identify correctly targeted clones is indicated. Cre expression in targeted ES cells leads to recombination between the two loxP sites and excision of the interjacent Neo cassette. (c) Southern blot from MfeI-digested ES cell DNA. The position of the probe used to detect 9.2 kb (+/+), 5.9 kb (Abl μ NLS neo) and 4 kb (Abl μ NLS) fragments is indicated in (b). (d) Expression of Abl and Abl μ NLS in ES cells. Abl protein was detected by immunoblot analysis from parental and targeted ES cells. An additional band reacting with monoclonal Abl antibody 8E9 was detected only in ES cells containing the neomycin cassette (arrowhead). (e) Abl subcellular localization in ES cells. ES cells were left untreated or treated with 10 nM LMB for 5 h to block nuclear export, and processed for indirect immunofluorescence. Merged deconvolution images show Abl staining in red, Hoechst (DNA) in blue, and phalloidin (Actin) in green

by polymerase chain reaction to contain the substitution mutations, denominated as the Abl μ NLS allele, which were also confirmed by Southern blotting (Figure 1c). Two heterozygous Abl $^{+/\mu$ NLS neo clones were converted to homozygosity by selection with high concentrations of neomycin (Figure 1c, lane 3). The neomycin cassette was then removed by the ectopic expression of Cre recombinase and correct excision was again confirmed by Southern blot (Figure 1c, lanes 4 and 5).

In ES cells homozygous for the Abl μ NLS allele, the mutant protein is expressed at a similar level as wild-type Abl (Figure 1d). The wild-type Abl protein is localized predominantly in the cytoplasm of ES cells (Figure 1e, top left panel). To determine if Abl enters the nucleus of ES cells, we used

Leptomycin B (LMB) to block the nuclear export of Abl.^{5,15} Following a 5-h incubation with LMB, nuclear accumulation of Abl was observed in wild-type ES cells (Figure 1e, top right panel). This result showed that Abl undergoes nucleo-cytoplasmic shuttling in ES cells with the dynamic equilibrium favoring nuclear export. Unlike wild-type Abl, the Abl μ NLS protein remained exclusively cytoplasmic irrespective of LMB treatment (Figure 1e, bottom panels). Thus, the knock-in mutations have indeed abolished the NLS function, and the Abl μ NLS protein is unable to shuttle between the cytoplasm and the nucleus.

DNA damage-induced nuclear accumulation of Abl in ES cells. Cisplatin, which is a chemotherapeutic drug widely

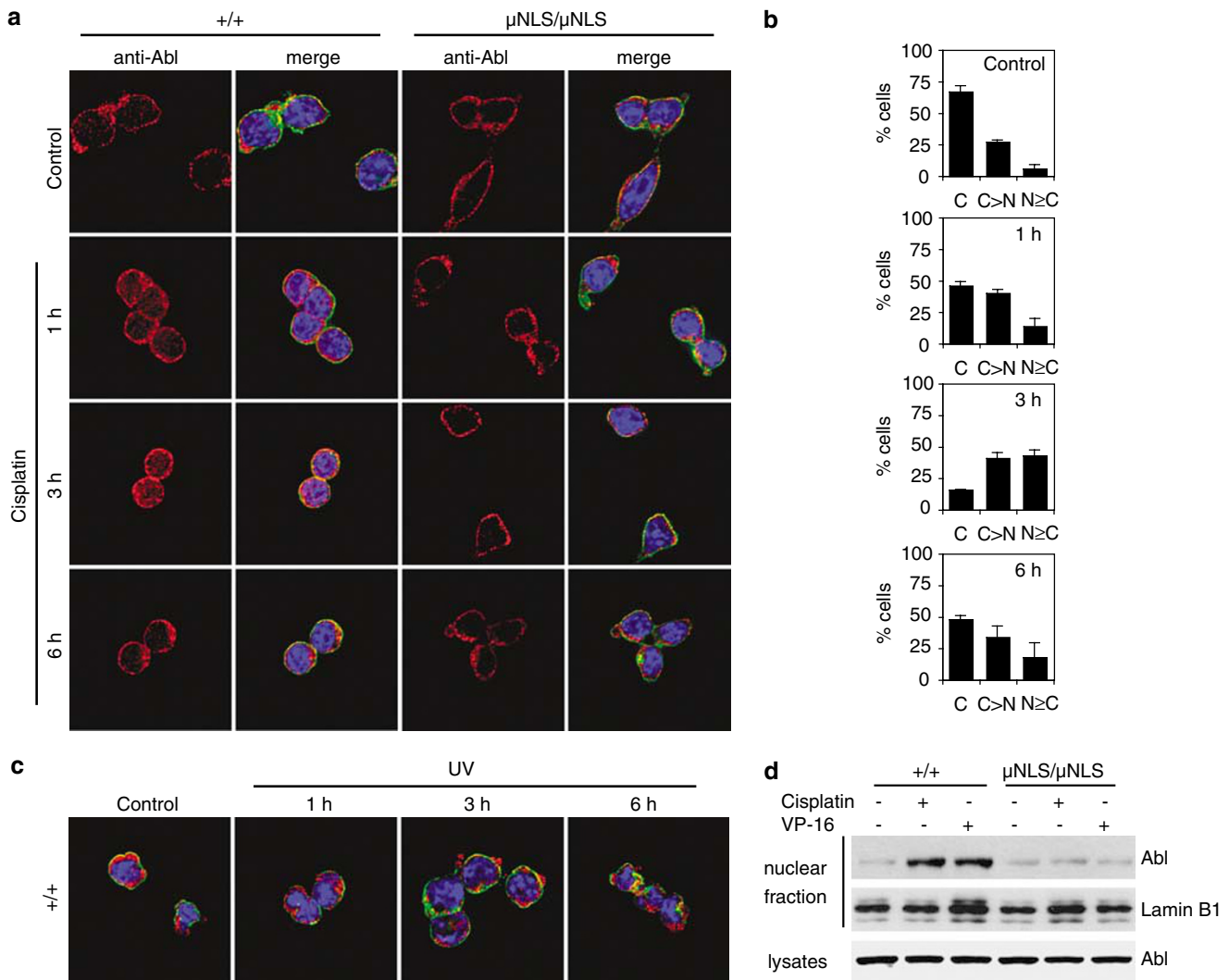


Figure 2 Nuclear accumulation of Abl in response to cisplatin but not UV. (a) Localization of Abl after cisplatin treatment. Parental (+/+) and *Abl* μ NLS (μ NLS/ μ NLS) ES cells were treated with 25 μ M cisplatin, fixed at the indicated time, and processed for indirect immunofluorescence. Deconvolution images of anti-Abl staining (red) are shown alone, and merged with images of DNA (blue) and actin (green). (b) Percentage of parental cells showing nuclear accumulation of Abl after cisplatin. Abl staining from 50 cells per slide was scored as cytoplasmic (C), stronger cytoplasmic than nuclear (C > N) or strong nuclear (N \geq C). Mean \pm standard deviation (S.D.) from two independent experiments is shown. (c) Abl localization after UV irradiation. Parental ES cells were subject to 30 J/m² UV, and the localization of Abl was examined at different time points by immunofluorescence. Merged deconvolution images show Abl staining in red, DNA (Hoechst) in blue and actin (Phalloidin) in green. (d) ES cells were exposed to 25 μ M cisplatin or 10 μ M etoposide (VP-16) for 3 h and nuclear fractionation performed as described in Material and Methods. Nuclear accumulation of Abl was detected by Western blot. Lamin B1 serves as loading control of the nuclear fraction

used in the treatment of testicular and ovarian cancer, has been shown to activate nuclear Abl tyrosine kinase.^{4,9,14} We found Abl to accumulate in the nuclei of ES cells at 1–3 h after cisplatin treatment (Figure 2a and b). At 6 h, Abl was mostly cytoplasmic again (Figure 2a and b). In accordance with the abrogation of its nuclear import by the μ NLS mutations, we did not detect nuclear accumulation of *Abl* μ NLS at any time after exposure to cisplatin (Figure 2a); nor did we detect nuclear accumulation of Abl at any time point after UV exposure (Figure 2c), in keeping with the previous finding that Abl is not activated by UV.⁹ The increase in the amount of nuclear Abl in +/+ ES cells after cisplatin or etoposide exposure was also observed in cell fractionation experiments (Figure 2d). In *Abl* μ NLS ES cells,

cisplatin or etoposide treatment did not alter the low level of *Abl* μ NLS that was found in the nuclear fraction most likely owing to trapping (Figure 2d). A previous report has shown that treatment of HeLa cells with adriamycin caused an increase in the levels of nuclear Abl.²⁰ We could not detect the nuclear accumulation of Abl by immunofluorescence staining of HeLa cells (Supplementary Figure 2), most likely because a considerable fraction of Abl is present in the nuclei of HeLa cells before adriamycin exposure (Supplementary Figure 2). Nevertheless, genotoxin-induced nuclear accumulation of Abl is readily detected by immunofluorescence staining and subcellular fractionation in mouse ES cells, and this response is blocked by the μ NLS knock-in mutations.

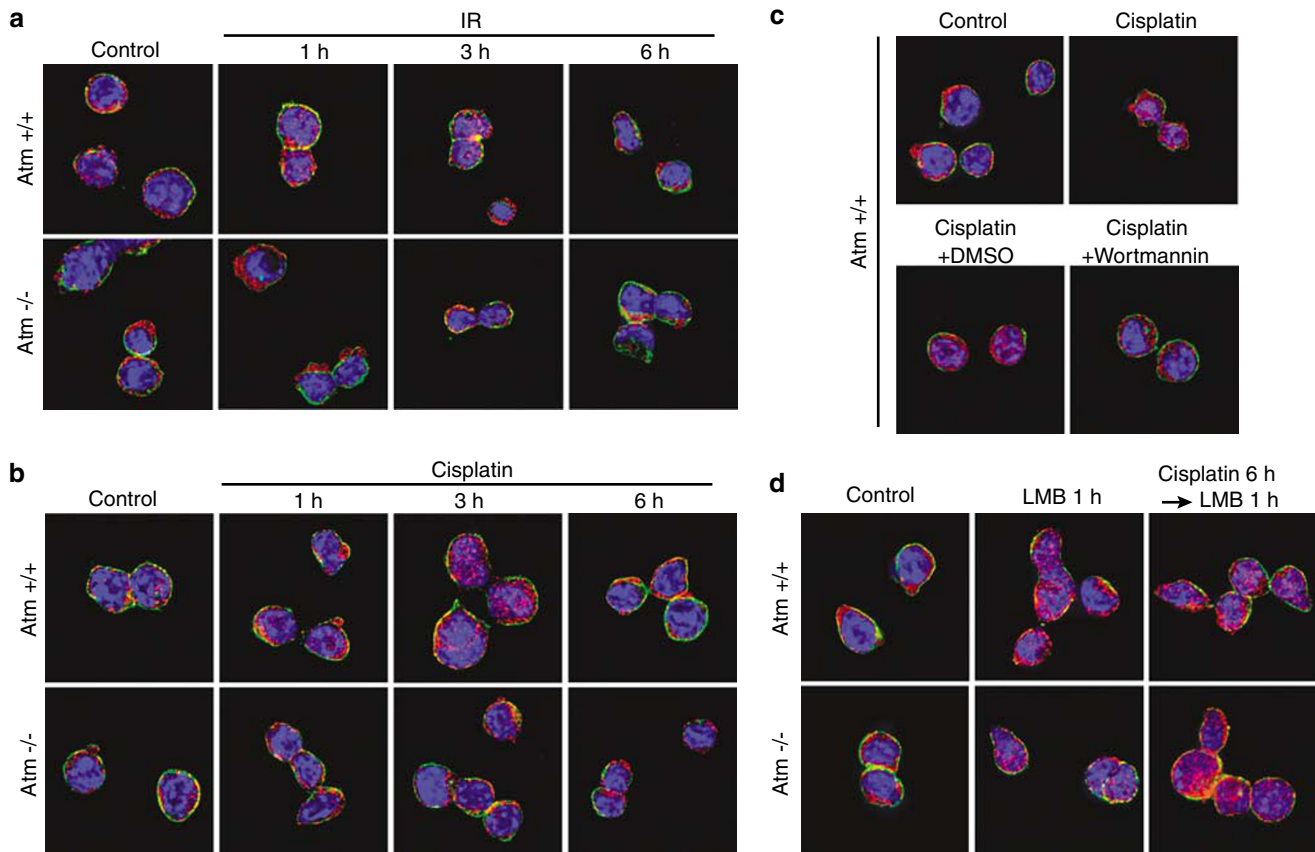


Figure 3 Abl localization in *Atm*^{-/-} ES cells. (a–d) Merged deconvolution images of Abl (red), DNA (blue) and actin (green) are shown. (a) Localization of Abl after IR. *Atm*^{+/+} and *Atm*^{-/-} ES cells were left untreated or irradiated with 10 Gy gamma irradiation and stained for immunofluorescence. (b) Localization of Abl after cisplatin treatment. ES cells were left untreated or treated with 25 μ M cisplatin, and fixed for immunofluorescence at the indicated times. (c) Wortmannin blocks nuclear accumulation of Abl. *Atm*^{+/+} ES cells were left untreated or treated with 25 μ M cisplatin alone, cisplatin plus solvent (DMSO), or cisplatin plus 20 μ M wortmannin for 3 h, and subsequently processed for immunofluorescence. (d) Shuttling of Abl in *Atm*^{-/-} cells. Subcellular localization of Abl in *Atm*^{+/+} and *Atm*^{-/-} ES cells was determined after 10 nM LMB treatment for 1 h or after 25 μ M Cisplatin for 6 h followed by LMB treatment for 1 h

ATM is necessary for Abl nuclear accumulation after DNA damage.

The ataxia telangiectasia mutated (ATM) kinase is an important transducer of DNA damage signals.²¹ The ATM function is required for IR to activate the Abl kinase.^{8,22} We therefore examined the nuclear accumulation of Abl in *Atm*^{+/+} and *Atm*^{-/-} ES cells after IR (Figure 3). In *Atm*^{+/+} ES cells, nuclear accumulation of Abl was observed between 1 and 3 h after IR (Figure 3a, upper panels). By 6 h, Abl was mostly cytoplasmic (Figure 3a, upper panels). In ES cells lacking the ATM kinase,²³ Abl did not accumulate in the nucleus after IR but remained predominantly cytoplasmic throughout the experimental time course (Figure 3a, lower panels). In unpublished results, our lab has found that ATM is also required for cisplatin to activate Abl tyrosine kinase (J Gong and JYJ Wang, unpublished). Consistent with this previous observation, we found cisplatin-induced nuclear accumulation of Abl was also abolished in *Atm*^{-/-} ES cells (Figure 3b, lower panels). Wortmannin, an inhibitor of PI(3) kinases including ATM,²⁴ also abrogated the cisplatin-induced nuclear accumulation of Abl (Figure 3c, lower right panel). ATM was not required for Abl nuclear import in the absence of genotoxins, because treatment of *Atm*^{-/-} cells with LMB trapped Abl in the nucleus either in the absence or

the presence of cisplatin (Figure 3d, lower panels). LMB-induced nuclear accumulation of Abl was observed in cisplatin-treated cells at a time (6 h) when Abl was mostly cytoplasmic (compare Figure 3d right-most panels with Figure 3b right-most panels), suggesting nucleocytoplasmic shuttling was not permanently altered by cisplatin. Thus, ATM is not required for Abl to enter the nuclear compartment, but it is necessary for Abl to accumulate in the nucleus following DNA damage.

Abl μ NLS ES cells show reduced apoptotic response to cisplatin, etoposide and IR but not UV.

We have found that early passage ES cell cultures are hypersensitive to cisplatin-induced DNA fragmentation. This ES cell trait is lost with manipulations such as longer passage time in culture and retroviral infections. In this study, we focused on the apoptotic response of early passage ES cells. At 18 h after the addition of cisplatin (25 μ M), DNA fragmentation was observed by flow cytometry in \sim 50% of the *Abl*^{+/+} ES cells and the fraction of sub-G1 DNA content increased to \sim 80% after 30 h (Figure 4a and b). In *Abl* μ NLS ES cells, a slower kinetics of DNA fragmentation was consistently observed (Figure 4a and b). The difference in the rate of DNA

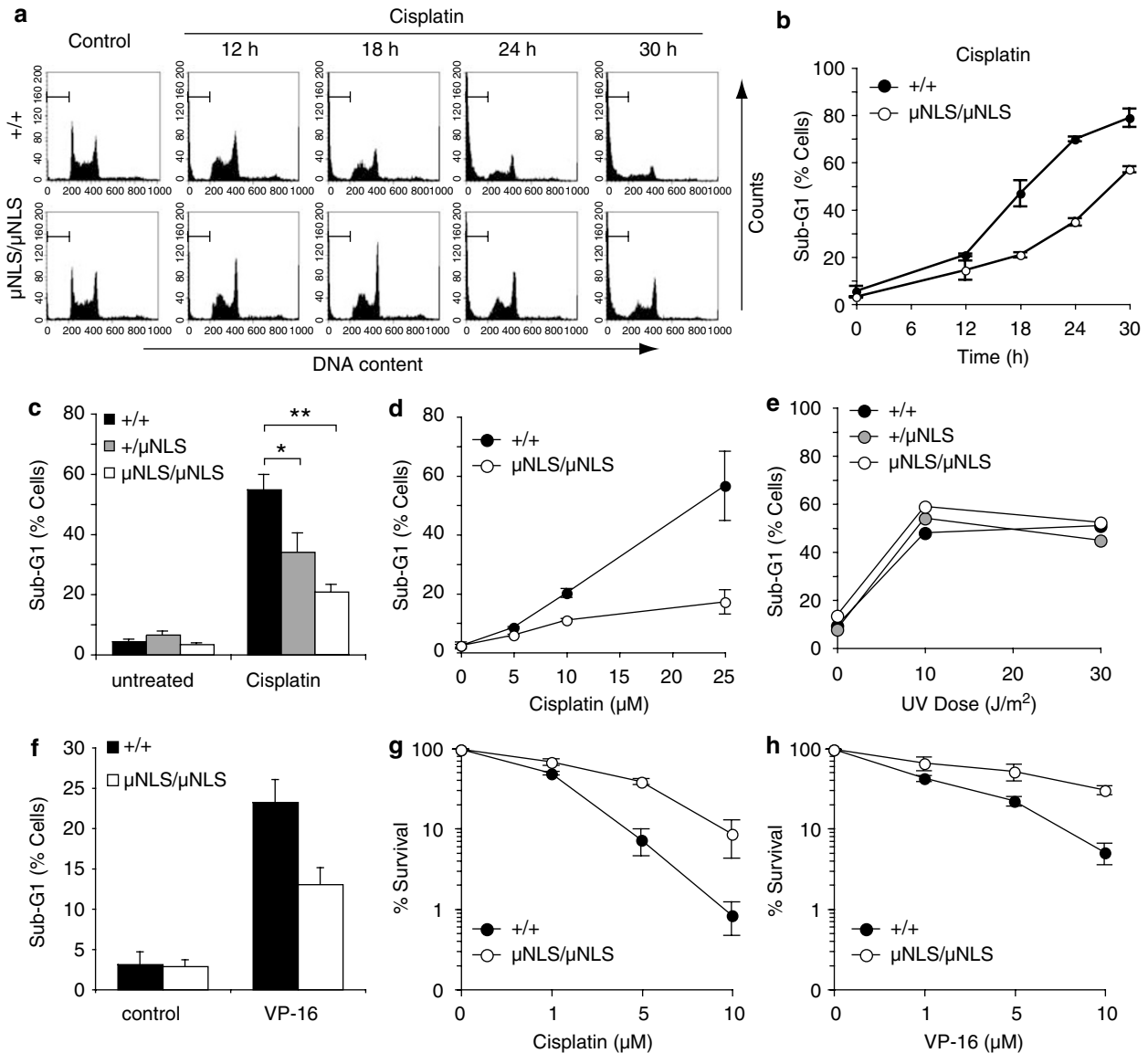


Figure 4 *Abi* μ NLS ES cells show reduced apoptosis in response to cisplatin but not UV. (a) Cisplatin-induced apoptosis in ES cells. Parental (+/+) and *Abi* μ NLS (μ NLS/ μ NLS) ES cells were treated with 25 μ M cisplatin for the indicated time. Sub-G1 DNA content indicating apoptosis was determined by propidium iodide staining and flow cytometry. (b) Graphical representation of the time course shown in (a). (c) Parental, +/ μ NLS and μ NLS/ μ NLS ES cells were treated with 25 μ M cisplatin for 18 h and analyzed for sub-G1 DNA content by flow cytometry. Mean \pm S.D. from three independent experiments is shown. (* P < 0.05; ** P < 0.01 determined by paired Student's *t*-test) (d) Dose–response to cisplatin. ES cells were exposed to different doses of cisplatin for 18 h and analyzed by flow cytometry. (e) Apoptosis after UV. ES cells were irradiated with different doses of UV at 254 nm and DNA fragmentation was determined by flow cytometry. (f) ES cells were treated with 10 μ M etoposide (VP-16) and the DNA content determined by flow cytometry after 18 h. Mean \pm S.D. from two independent experiments is shown. (g and h) ES cells were treated with different doses of cisplatin (g) or etoposide (h) and clonogenic survival was determined as described in Materials and Methods. Mean \pm S.D. from two independent experiments are shown

fragmentation between +/+ and μ NLS/ μ NLS cells was statistically significant (Figure 4c), and observed at several concentrations of cisplatin (Figure 4d). The heterozygous +/ μ NLS cells showed an intermediate response, which was also significantly different from +/+ cells (Figure 4c). Similarly, we found etoposide-induced DNA fragmentation to be reduced in the *Abi* μ NLS ES cells relative to their *Abi*^{+/+} counterparts (Figure 4f). By contrast, we found no difference in the apoptotic response of +/+, +/ μ NLS and μ NLS/ μ NLS ES cells to UV irradiation (Figure 4e). Consistent with the reduced apoptotic

response, clonogenic survival of the *Abi* μ NLS ES cells was significantly increased relative to the *Abi*^{+/+} ES cells following exposure to either cisplatin (Figure 4g) or etoposide (Figure 4h).

Reduced caspase activation despite normal p53 response in *Abi* μ NLS ES cells. The accumulation of p53 protein was observed in cisplatin-treated *Abi*^{+/+} and *Abi* ^{μ NLS/ μ NLS} ES cells (Figure 5a). The C-terminal acetylation (Figure 5b) and Ser-18 phosphorylation (Figure 5c) of p53 were also similarly induced by cisplatin

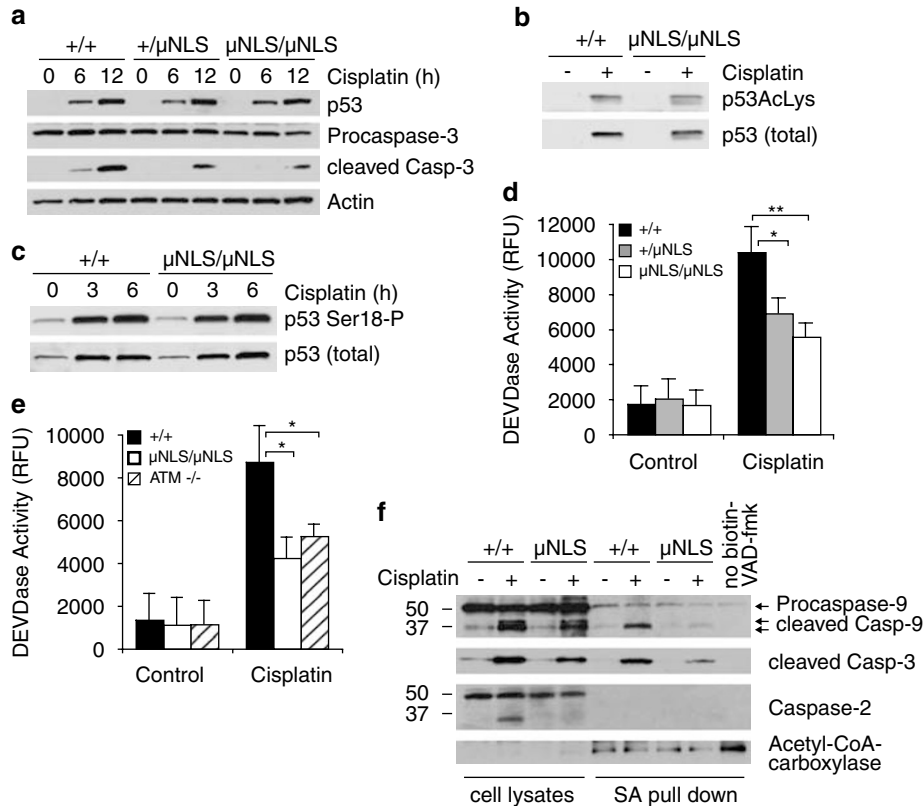


Figure 5 Decreased caspase activation in *Abli* μ NLS ES cells. (a) p53 stabilization and caspase-3 cleavage. Parental, $+/\mu$ NLS and μ NLS/ μ NLS cells were treated with 25 μ M cisplatin for the indicated time. Cell lysates were immunoblotted with antibodies against p53, procaspase-3 and cleaved (active) caspase-3. Actin served as loading control. (b and c) p53 post-translational modification. ES cells were treated with cisplatin for 6 h and the levels of Lys acetylation (b) and Ser-18 phosphorylation (c) determined by Western blot. (d) Caspase-3 activation after cisplatin. ES cells were treated with cisplatin for 12 h and caspase activity determined in lysates using z-DEVD-AMC as substrate. Mean \pm S.D. from four independent experiments is shown ($*P < 0.05$; $**P < 0.01$ determined by paired Student's *t*-test). (e) Caspase-3 activity in *Atm* $^{-/-}$ ES cells. Parental, *Abli* μ NLS/ μ NLS and *Atm* $^{-/-}$ cells were treated with 25 μ M cisplatin for 12 h and DEVDase activity measured *in vitro*. Mean \pm S.D. from three independent experiments is shown ($*P < 0.05$). (f) *In vivo* caspase labeling. ES cells were pretreated for 1 h with 50 μ M biotin-VAD-fmk and then exposed to cisplatin for 6 h in the presence of biotin-VAD-fmk. Biotinylated proteins were precipitated with streptavidine (SA) sepharose beads and separated by SDS-PAGE. Immunoblots were probed with antibodies against caspase-9, cleaved caspase-3 and caspase-2. Biotinylated acetyl-CoA-carboxylase served as loading control. The position of molecular weight standards (kDa) is indicated

in $+/+$ and μ NLS/ μ NLS ES cells. Thus, nuclear import of Abl is not required for cisplatin to activate p53 in ES cells. Previous experiments conducted with somatic cell lines have shown that Abl activates the proapoptotic activity of p73.^{4,12,25} We have not been able to detect the p73 protein in mouse ES cells either in the absence or presence of DNA damage (data not shown). Thus, we cannot assess the contribution of p73 to DNA damage-induced apoptosis in ES cells. Despite the similar rates of p53 accumulation and post-translational modification, $+/\mu$ NLS and μ NLS/ μ NLS ES cells showed a delay in the processing of procaspase-3 relative to their *Abli* $^{+/+}$ counterparts (Figure 5a). We measured caspase activity using the fluorogenic substrate DEVD-AMC in the lysates of ES cells after 12 h of cisplatin treatment, and found significantly reduced DEVDase activities in $+/\mu$ NLS, μ NLS/ μ NLS and *Atm* $^{-/-}$ ES cells relative to their wild-type counterparts (Figure 5d and e, and Supplementary Figure 3). The reduced activation of caspase by cisplatin was observed in two independently derived *Abli* μ NLS ES cell clones (Supplementary Figure 3). The slower kinetics of caspase activation was also observed following exposure of μ NLS/ μ NLS ES cells to IR or etoposide

(Supplementary Figure 3), but not after UV treatment (data not shown).

Genotoxin-induced apoptosis is abrogated in ES cells by the knockout of either *Apaf-1* or *caspase-9*, demonstrating the apoptosome to be required for the apoptotic response of ES cells to DNA damage.^{16,17} We adopted a recently described *in vivo* caspase labeling protocol²⁶ to further examine the activation of apical caspases in ES cells (Figure 5f). Using a biotinylated general caspase inhibitor Val-Ala-Asp-fluoromethyl ketone (biotin-VAD-fmk) to covalently label active caspases with biotin, we were able to detect the auto-processed form of caspase-9²⁷ in streptavidin-sepharose precipitates from cisplatin-treated $+/+$ ES cells, with *Abli* μ NLS cells showing a decreased level of active caspase-9 (Figure 5f). Although a lower molecular weight caspase-2 band was observed in cisplatin-treated $+/+$ cells, we could not detect active caspase-2 by this biotin-VAD-fmk affinity-labeling method in $+/+$ or *Abli* μ NLS ES cells (Figure 5f). We were able to detect the large subunit of cleaved caspase-3 in the streptavidin precipitates, and the amount of active caspase-3 was again found to be lower in *Abli* μ NLS ES cells than that in $+/+$ ES cells (Figure 5f).

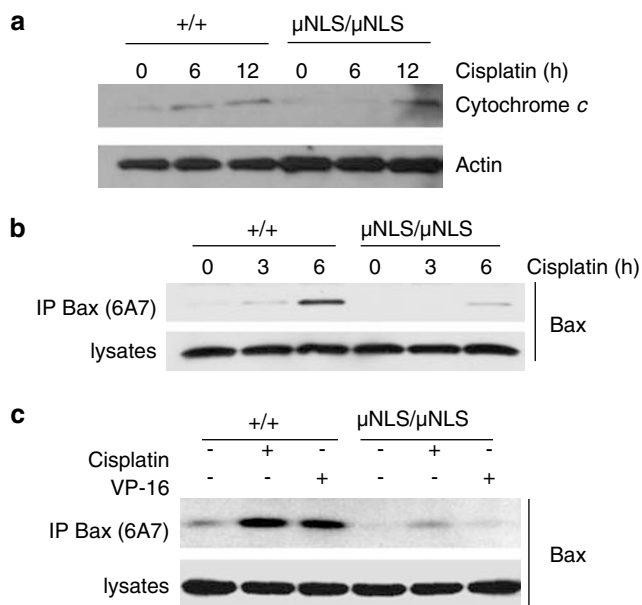


Figure 6 Bax conformational transition and cytochrome *c* release after cisplatin. (a) Cytochrome *c* release. ES cells were treated for 6 or 12 h with cisplatin and cytoplasmic extracts were prepared as described in Materials and Methods. The amounts of cytoplasmic cytochrome *c* and actin were determined by immunoblotting. (b) Time course of Bax activation. ES cells were treated with cisplatin for the indicated time and active Bax immunoprecipitated from lysates with monoclonal antibody 6A7. (c) Bax activation by cisplatin and etoposide. ES cells were treated as indicated for 6 h and active Bax was immunoprecipitated. Bax immunoblots from precipitates and lysates are shown

Delayed Bax-activation and cytochrome *c* release in *Abl* μ NLS cells. The activation of the apoptosome requires cytochrome *c* release from the mitochondria.¹ Consistent with the delayed activation of caspases in *Abl* μ NLS ES cells, we found that the appearance of cytosolic cytochrome *c* after cisplatin addition was delayed relative to the *Abl*^{+/+} ES cells by about 6 h (Figure 6a). It is well established that oligomerization of the proapoptotic multi-domain protein Bax in the mitochondrial outer membrane causes the leakage of cytochrome *c*.^{28,29} An important step in the activation of Bax is a conformational transition that exposes an N-terminal epitope,^{30,31} which can be detected by the monoclonal antibody 6A7. Following exposure to cisplatin, Bax conformational transition was detectable at 3 h and increased with time of treatment in *+/+* ES cells (Figure 6b). With the μ NLS/ μ NLS ES cells, Bax conformational transition became detectable only after 6 h of treatment (Figure 6b). The reduced activation of Bax was also observed in etoposide-treated *Abl* μ NLS ES cells at 6 h (Figure 6c), consistent with the delay in caspase activation (Supplementary Figure 3).

Cisplatin-induced ES cell apoptosis does not require transcription or Abl kinase activity. Previous studies with somatic cell lines have linked DNA damage-induced activation of Abl tyrosine kinase to the stabilization and activation of p73, which stimulates apoptosis through transactivation of Puma, p53AIP and possibly other proapoptotic genes.^{4,12,14} We inhibited transcription with

5,6-dichloro-1- β -D-ribofuranosylbenzimidazole riboside (DRB), which interferes with the phosphorylation of RNA polymerase II C-terminal repeated domain and thus blocks transcription elongation.³² The amount of p53 protein increased upon treatment with DRB in both the *Abl*^{+/+} and μ NLS/ μ NLS cells (Figure 7a). However, DRB did not affect cisplatin-induced processing of caspase-9 and caspase-3 (Figure 7a) nor did it affect the DEVDase activity in *+/+* or μ NLS/ μ NLS cells (data not shown). Thus, *Abl*/p73-dependent upregulation of gene expression does not appear to be required for cisplatin-induced apoptosis of ES cells.

Previous studies have shown that genotoxin-induced apoptosis in somatic cell lines is reduced by treatment with imatinib mesylate, which inhibits Abl tyrosine kinase.^{4,12,14} We thus examined whether inhibition of Abl kinase could affect cisplatin-induced ES cells apoptosis. We treated ES cells with two kinase inhibitors, STI571 (a.k.a. imatinib mesylate, GleevecTM) and PD166326, and found neither to interfere with cisplatin-induced caspase activation in *+/+* or μ NLS/ μ NLS (Figures 7b and c). Inhibitors of Abl kinase also had no effect on the DNA fragmentation in cisplatin-treated *+/+* or μ NLS/ μ NLS cells (Figure 7d). These results suggest that cisplatin-induced apoptosis in ES cells does not depend on ongoing transcription or Abl kinase activity.

Discussion

Regulated nuclear-cytoplasmic transport is an important mechanism of signal transduction, of which defects have been detected in many cancer cells.³³ DNA damage-induced nuclear accumulation of Abl shown here in mouse ES cells has also been observed with HeLa cells.²⁰ Abl nuclear accumulation may be the result of increased import, nuclear retention or decreased export. In HeLa cells, DNA damage stimulates the nuclear import of Abl by causing its release from cytoplasmic 14-3-3-proteins through a JNK-dependent pathway.²⁰ In ES cells, we have observed nuclear accumulation of Abl after IR or cisplatin treatment but not after exposure to UV, which is a potent activator of JNKs.^{34,35} Thus, JNK-dependent and 14-3-3-mediated regulation of Abl nuclear import may be absent from ES cells. It is possible that DNA damage may induce the nuclear retention of Abl in ES cells, as suggested by the requirement for ATM in Abl nuclear accumulation. Previous studies have shown Abl to bind ATM,^{8,22} DNA-PK,³⁶ and BRCA1.³⁷ The phosphorylation of Abl by ATM at an SQ-site^{4,8} could conceivably allow for Abl interaction with a phospho-serine binding domain, leading to nuclear retention. Irrespective of the mechanism, our results have established that the transient nuclear accumulation of Abl contributes to DNA damage-induced activation of Bax.

Previous knockout studies have demonstrated the requirement for Apaf-1 and caspase-9 in genotoxin- or UV-induced apoptosis of ES cells and somatic cells.^{16,17} We show here that cisplatin induces phosphorylation, acetylation and accumulation of the p53 protein in ES cells (Figure 5), also similar to the observations made in somatic cells. However, pharmacological inhibition of RNA polymerase II-dependent transcription elongation does not abolish cisplatin-induced

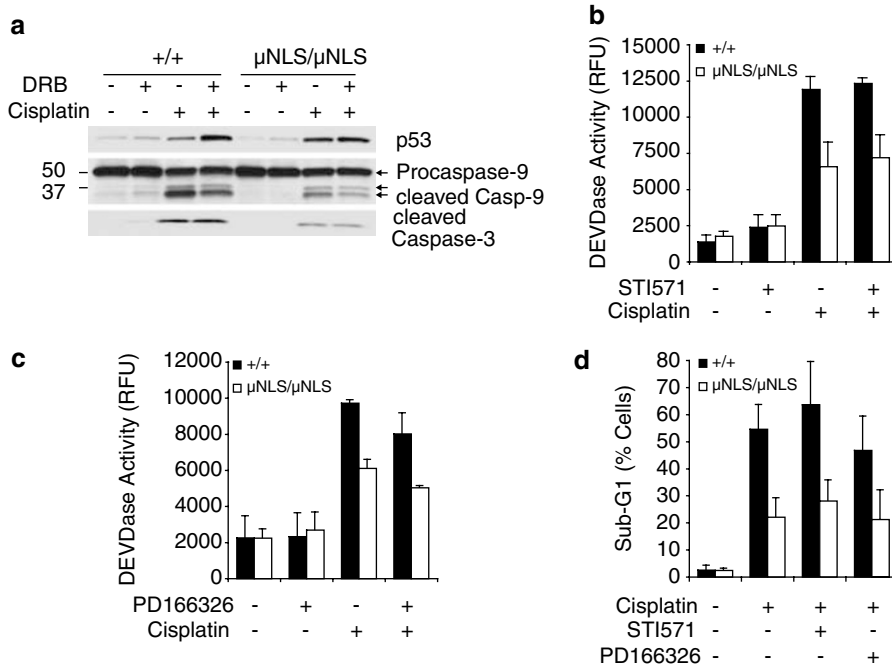


Figure 7 Inhibitors of transcription or Abl kinase do not block cisplatin-induced ES-cell apoptosis. (a) ES cells were treated with 30 μ M DRB and/or 25 μ M cisplatin for 12 h as indicated. The levels of p53, caspase-9 and cleaved caspase-3 were determined by immunoblotting. (b and c) *In vitro* caspase activity assays. +/+ and μ NLS/ μ NLS ES cells were pretreated with Abl kinase inhibitors 10 μ M STI571 (b) or 10 nM PD166326 (c) for 4 h followed by combined treatment with kinase inhibitor and 25 μ M cisplatin for 12 h. DEVDase activity was determined fluorimetrically in cell lysates. Results represent the mean from two independent experiments. (d) ES cells were treated with Abl kinase inhibitors and cisplatin as in (b) and sub-G1 DNA content determined by flow cytometry after 18 h. Mean \pm S.D. from three independent experiments are shown

apoptosis in ES cells (Figure 7). It has been reported that p53 is mostly localized to the cytoplasm of ES cells.³⁸ Together, these observations suggest that p53-mediated transactivation of BH3-domain proteins, for example, Puma and Noxa,^{39,40} may be dispensable for DNA damage-induced apoptosis in ES cells. Recent studies have suggested that p53 can directly interact with the antiapoptotic Bcl2-family proteins to promote cytochrome *c* release.^{2,41} This non-transcriptional mechanism of p53-dependent apoptosis may be the predominant pathway in ES cells.

Previous studies have shown Abl tyrosine kinase to stimulate p73-dependent trans-activation of Puma and p53AIP1, thereby contributing to p53-independent apoptosis.^{4,12} As transcription is dispensable for DNA damage-induced apoptosis in ES cells, the Abl/p73 proapoptotic pathway may only be relevant in somatic cells. Furthermore, we found that inhibitors of Abl tyrosine kinase did not interfere with cisplatin-induced apoptosis in ES cells, suggesting Abl can stimulate mitochondria-dependent apoptosis through a kinase-independent mechanism. A recent report has shown that Abl, but not its kinase activity, can stimulate the degradation of UV-DDB2 by the Cul4A E3 ubiquitin ligase complex, resulting in inhibition of the global genome repair of UV-induced damage.⁴² In ES cells, nuclear translocation of Abl is not required for UV-induced apoptosis (Figure 4). However, it is possible that nuclear Abl protein may stimulate the degradation of other repair proteins to promote the accumulation of damaged DNA. In the absence of nuclear Abl, the accumulation of damage signals may be slower, leading to the delay in Bax activation.

Our findings may also be explained by another possibility, that is, the cytoplasmic Abl may protect against Bax activation in ES cells. In this scenario, DNA damage-induced nuclear accumulation of Abl only serves to remove it from the cytoplasm, thus allowing for a more efficient activation of Bax. The antiapoptotic function of Abl has been observed in *C. elegans*, where genetic ablation of the worm *abl* sensitizes the germ cells to IR-induced and p53-dependent apoptosis.⁴³ We are currently working on the creation of mice expressing the *Ab* μ NLS allele. Analyses of the death response in the tissues of the *Ab* μ NLS mice will yield further insight into the *in vivo* relevance of Abl nuclear import in genotoxin-induced apoptosis.

Materials and Methods

Plasmid construction. We constructed a targeting vector containing exon 11 and flanking sequences, and replaced the NLSs with the mutated sequence. An 11.4 kb fragment containing exon 11 of the mouse *abl1* gene was subcloned into pBluescript (Stratagene, La Jolla CA, USA) by recombinering⁴⁴ (Supplementary Figure 1). The region containing the three NLSs was replaced with the mutated cDNA and an *MfeI* restriction site in the 3' untranslated region was constructed by site-directed mutagenesis. A *loxP* flanked *PGK/Neo* cassette was placed into the intron preceding exon 11. All PCR amplified regions were sequenced for integrity.

Generation of *Ab* μ NLS/ μ NLS ES cells. TC-1 ES cells were cultured on a feeder layer of mitomycin C-inactivated primary fibroblasts in Dulbecco's modified Eagle's medium with Glutamax and high glucose (GIBCO/Invitrogen, Carlsbad, CA, USA) supplemented with 15% fetal bovine serum and recombinant LIF (Chemicon, Temecula, CA, USA). Ten micrograms of *EcoRV*-linearized targeting vector were electroporated into 2×10^7 ES cells. Positively targeted ES clones were identified by PCR with primers 'a' (5'-ATT GCT TAG ACA AGC CGA AAG CTG) and 'n' (5'-ATC AGG ATG ATC TGG ACG AAG AGC) and confirmed by non-radioactive

Southern blot (DIG High Prime DNA Labeling and Detection Kit II, Roche, Indianapolis, IN, USA) of *MfeI* digested genomic DNA. Heterozygous ES cells were converted to homozygosity by selection in 2.5–5 mg/ml G418 for 6 days.

Immunofluorescence. Feeder cells were removed by differential adhesion and ES cells were seeded onto gelatinized cover slips, allowed to attach for several hours and then treated with drugs. Cells were fixed in 4% formaldehyde, permeabilized with 0.3% Triton X-100 in PBS, blocked with 10% normal goat serum in PBS, and incubated with anti-Abl antibody (8E9, Pharmingen/Invitrogen, Carlsbad, CA, USA) for 1 h. Cells were then incubated with Alexa Fluor 568-conjugated secondary antibodies (goat anti-mouse Fab fragment, Molecular Probes/Invitrogen, Carlsbad, CA, USA) and Alexa Fluor 488-conjugated Phalloidin (Molecular Probes) for 1 h. Nuclei were counterstained with Hoechst 33258 (Molecular Probes) and coverslips mounted onto glass slides with gel mount (Biomed, Foster City, CA, USA). Images were captured with a DeltaVision Restoration microscope system. Approximately 30 optical sections (0.3 μ m) were taken and enhanced using Delta Vision's deconvolution process. Scoring of nuclear versus cytoplasmic intensity was performed on a Nikon microscope equipped with a \times 0.60 HRD060-NIK CCD camera (Diagnostic Instruments, Sterling Heights, MI, USA). Images were acquired with the \times 100 lens and intensity was scored based on the Surface Plot function of Image-Pro Plus 3.0 software (Media Cybernetics, Silver Spring, MD, USA). A total 50 cells per slide from two independent experiments were scored. The scoring was carried out blind to treatment status of samples.

Subcellular fractionation. ES cells were suspended in fractionation buffer (250 mM glucose, 10 mM Tris/HCl pH 7.4, 10 mM KCl, 1.5 mM MgCl₂, 1 mM EDTA, 1 mM EGTA, 1 mM dithiothreitol, 0.1 mM phenylmethylsulfonylfluoride) containing protease inhibitor cocktail (Roche), and disrupted by 70 strokes through a Dounce homogenizer. The homogenate was centrifuged at 60 \times g to remove intact cells, and the supernatant was further contributed at 600 \times g to collect the nuclear pellet. The levels of Abl in whole cell lysates and nuclear lysates were determined by immunoblotting with monoclonal antibody 8E9.

FACS analysis. ES cells (3 \times 10⁵) per well were seeded in six-well plates, grown for 24 h and then treated as indicated. Adherent cells were collected by trypsinization and pooled with floating cells, washed with PBS containing 1% FBS and stained with Propidium Iodide solution (0.1% Triton X-100, 1 mM Tris/HCl pH8, 0.1 mM EDTA, 0.1% Na-Citrate, 50 μ g/ml propidium iodide, 50 ng/ml RNAse A) for at least 1 h at 4°C. Sub-G1 DNA content was determined on a FACSCalibur flow cytometer (Becton Dickinson, Franklin Lakes, NJ, USA) with CellQuest software.

Clonogenic survival assay. *Abl*^{+/+} and *Abl*^{NLS/ μ NLS} ES cells were plated on mouse embryonic fibroblast feeder layers in six-well plates at a density of 1 \times 10³ cells/well a day before treatment. ES cells were exposed to different doses of CDDP or Etoposide for 1 h. Cells were then washed and cultured in complete media in the absence of drugs with fresh media provided every 48 h. After 8 days of culture, colonies were fixed and stained with 0.25% crystal violet, and the ratio of the number of surviving colonies in the treated sample to those in the untreated control was calculated.

Caspase-3 activity assay. Caspase-3 activity was measured with the EnzCheck Caspase-3 assay kit no. 1 (Molecular Probes) according to the manufacturer's instructions. Samples were analyzed in 96-well plates in triplicate using 25 μ g total protein per reaction. Plates were incubated at room temperature in the dark and emission at 441 nm after excitation at 352 nm was quantified on a Spectramax Gemini Microplate reader (Molecular Devices, Sunnyvale, CA, USA). Multiple readings were performed over time to ensure linearity.

Western blotting. Cells were seeded on gelatinized 60 mm dishes, grown for 24 h and then treated as indicated. Floating and adherent cells were collected and lysed in RIPA buffer (150 mM NaCl, 50 mM Tris pH 7.4, 0.1% SDS, 1% NP-40, 0.25% sodium deoxycholate, 1 mM EDTA, 1 mM EGTA) with complete protease inhibitor cocktail (Roche) and 1 mM PMSF. Protein concentration was determined with the DC Protein assay (Biorad, Hercules, CA, USA). Antibodies used were 8E9 (Pharmingen) against Abl, PAB240 (Zymed/Invitrogen, Carlsbad, CA, USA) against p53, polyclonal phospho-p53 against Ser-18 phosphorylated p53 (no. 9284, Cell Signaling, Danvers, MA, USA), 8G10 and Asp175 (Cell Signaling) against Caspase-3, AC-40 (Sigma, St. Louis, MO, USA) against actin and MAB3213 (Upstate/

Millipore, Billerica, MA, USA) against nuclear lamin B1. The antibody for acetylated p53 was a generous gift of Dr Wei Gu (Columbia University).⁴⁵ Immunoblots were developed with SuperSignal West (Pierce, Rockford, IL, USA). For detection of cytochrome c release, cells were suspended in lysis buffer (210 mM Mannitol, 70 mM Sucrose, 10 mM HEPES/KOH pH7.4, 0.5 mM EGTA, 4 mM MgCl₂, 5 mM Na₂HPO₄) and broken up by 20 strokes through a 25-gauge needle. Heavy membrane fractions were pelleted for 10 min at 4°C, and supernatants used for Western blot. Cytochrome c was detected with monoclonal antibody 7H8.2C12 (Pharmingen).

In vivo caspase labeling. ES cells were pre-incubated with 50 μ M biotin-VAD-fmk (Kamiya Biomedical Company, Seattle, WA, USA) for 1 h, followed by 25 μ M cisplatin for 6 h in the presence of biotin-VAD-fmk. Cells were then washed and lysed in RIPA buffer as described above. Total protein (700 μ g) was used for pull-down assays with 88 μ l streptavidin sepharose (Amersham Biosciences, Piscataway, NJ, USA) at 4°C over night. Beads were washed five times in lysis buffer and boiled in SDS sample buffer to elute bound proteins. Aliquots from whole-cell lysate and pull down were separated by SDS-PAGE and probed with antibodies against caspase-9 (no. 9508), cleaved caspase-3 (Asp175), Acetyl CoA carboxylase (all from Cell Signaling) and 11B4 against caspase-2 (Alexis, San Diego, CA, USA).

Bax immunoprecipitation. ES cells were lysed for 30 min on ice in IP buffer (10 mM HEPES/KOH pH7.4, 150 mM NaCl, 1% CHAPS) containing complete protease inhibitor cocktail (Roche) and 1 mM PMSF. Total protein (300 μ g) was used for immunoprecipitations with 1 μ g monoclonal anti-Bax antibody 6A7 (Trevigen, Gaithersburg, MD, USA), which recognizes the exposed N-terminus, for 2 h at 4°C. Immunocomplexes were captured with 40 μ l protein-G sepharose beads 1 h at 4°C and washed three times in lysis buffer. Immunocomplexes were broken up by boiling in SDS sample buffer and aliquots analyzed by immunoblot with monoclonal anti-Bax antibody 5B7 (Trevigen).

Acknowledgements. We thank Dr J Feramisco and M Szeszel for assistance with deconvolution microscopy and Wei Gu for the antibody against acetylated p53. MP was supported by DOC (DOCTORAL SCHOLARSHIP PROGRAMME OF THE AUSTRIAN ACADEMY OF SCIENCES). This work was supported by a grant (CA43054) from the National Cancer Institute, USA, to JYJW.

1. Wang X. The expanding role of mitochondria in apoptosis. *Genes Dev* 2001; **15**: 2922–2933.
2. Chipuk JE, Kuwana T, Bouchier-Hayes L, Droin NM, Newmeyer DD, Schuler M *et al*. Direct activation of Bax by p53 mediates mitochondrial membrane permeabilization and apoptosis. *Science* 2004; **303**: 1010–1014.
3. Wang JY, Cho SK. Coordination of repair, checkpoint, and cell death responses to DNA damage. *Adv Protein Chem* 2004; **69**: 101–135.
4. Gong JG, Costanzo A, Yang HQ, Melino G, Kaelin Jr WG, Levvero M *et al*. The tyrosine kinase c-Abl regulates p73 in apoptotic response to cisplatin-induced DNA damage. *Nature* 1999; **399**: 806–809.
5. Taagepera S, McDonald D, Loeb JE, Whitaker LL, McElroy AK, Wang JY *et al*. Nuclear-cytoplasmic shuttling of C-ABL tyrosine kinase. *Proc Natl Acad Sci USA* 1998; **95**: 7457–7462.
6. Woodring PJ, Hunter T, Wang JY. Regulation of F-actin-dependent processes by the Abl family of tyrosine kinases. *J Cell Sci* 2003; **116**: 2613–2626.
7. Welch PJ, Wang JY. A C-terminal protein-binding domain in the retinoblastoma protein regulates nuclear c-Abl tyrosine kinase in the cell cycle. *Cell* 1993; **75**: 779–790.
8. Baskaran R, Wood LD, Whitaker LL, Canman CE, Morgan SE, Xu Y *et al*. Ataxia telangiectasia mutant protein activates c-Abl tyrosine kinase in response to ionizing radiation. *Nature* 1997; **387**: 516–519.
9. Liu ZG, Baskaran R, Lea-Chou ET, Wood LD, Chen Y, Karin M *et al*. Three distinct signalling responses by murine fibroblasts to genotoxic stress. *Nature* 1996; **384**: 273–276.
10. Yuan ZM, Shioya H, Ishiko T, Sun X, Gu J, Huang YY *et al*. p73 is regulated by tyrosine kinase c-Abl in the apoptotic response to DNA damage. *Nature* 1999; **399**: 814–817.
11. Agami R, Blandino G, Oren M, Shaul Y. Interaction of c-Abl and p73alpha and their collaboration to induce apoptosis. *Nature* 1999; **399**: 809–813.
12. Melino G, Bernassola F, Ranalli M, Yee K, Zong WX, Corazzari M *et al*. p73 Induces apoptosis via PUMA transactivation and Bax mitochondrial translocation. *J Biol Chem* 2004; **279**: 8076–8083.
13. Vella V, Zhu J, Frasca F, Li CY, Vigneri P, Vigneri R *et al*. Exclusion of c-Abl from the nucleus restrains the p73 tumor suppression function. *J Biol Chem* 2003; **278**: 25151–25157.

14. Truong T, Sun G, Doorly M, Wang JY, Schwartz MA. Modulation of DNA damage-induced apoptosis by cell adhesion is independently mediated by p53 and c-Abl. *Proc Natl Acad Sci USA* 2003; **100**: 10281–10286.
15. Vigneri P, Wang JY. Induction of apoptosis in chronic myelogenous leukemia cells through nuclear entrapment of BCR-ABL tyrosine kinase. *Nat Med* 2001; **7**: 228–234.
16. Yoshida H, Kong YY, Yoshida R, Elia AJ, Hakem A, Hakem R *et al*. Apaf1 is required for mitochondrial pathways of apoptosis and brain development. *Cell* 1998; **94**: 739–750.
17. Hakem R, Hakem A, Duncan GS, Henderson JT, Woo M, Soengas MS *et al*. Differential requirement for caspase 9 in apoptotic pathways *in vivo*. *Cell* 1998; **94**: 339–352.
18. Corbet SW, Clarke AR, Gledhill S, Wyllie AH. P53-dependent and -independent links between DNA-damage, apoptosis and mutation frequency in ES cells. *Oncogene* 1999; **18**: 1537–1544.
19. Wen ST, Jackson PK, Van Etten RA. The cytostatic function of c-Abl is controlled by multiple nuclear localization signals and requires the p53 and Rb tumor suppressor gene products. *EMBO J* 1996; **15**: 1583–1595.
20. Yoshida K, Yamaguchi T, Natsume T, Kufe D, Miki Y. JNK phosphorylation of 14-3-3 proteins regulates nuclear targeting of c-Abl in the apoptotic response to DNA damage. *Nat Cell Biol* 2005; **7**: 278–285.
21. Shiloh Y. ATM and related protein kinases: safeguarding genome integrity. *Nat Rev Cancer* 2003; **3**: 155–168.
22. Shafman T, Khanna KK, Kedar P, Spring K, Kozlov S, Yen T *et al*. Interaction between ATM protein and c-Abl in response to DNA damage. *Nature* 1997; **387**: 520–523.
23. Xu Y, Ashley T, Brainerd EE, Bronson RT, Meyn MS, Baltimore D. Targeted disruption of ATM leads to growth retardation, chromosomal fragmentation during meiosis, immune defects, and thymic lymphoma. *Genes Dev* 1996; **10**: 2411–2422.
24. Chan DW, Son SC, Block W, Ye R, Khanna KK, Wold MS *et al*. Purification and characterization of ATM from human placenta. A manganese-dependent, wortmannin-sensitive serine/threonine protein kinase. *J Biol Chem* 2000; **275**: 7803–7810.
25. Costanzo A, Merlo P, Pediconi N, Fulco M, Sartorelli V, Cole PA *et al*. DNA damage-dependent acetylation of p73 dictates the selective activation of apoptotic target genes. *Mol Cell* 2002; **9**: 175–186.
26. Tu S, McStay GP, Boucher LM, Mak T, Beere HM, Green DR. *In situ* trapping of activated initiator caspases reveals a role for caspase-2 in heat shock-induced apoptosis. *Nat Cell Biol* 2006; **8**: 72–77.
27. Srinivasula SM, Ahmad M, Fernandes-Alnemri T, Alnemri ES. Autoactivation of procaspase-9 by Apaf-1-mediated oligomerization. *Mol Cell* 1998; **1**: 949–957.
28. Annis MG, Soucie EL, Dlugosz PJ, Cruz-Aguado JA, Penn LZ, Leber B *et al*. Bax forms multispanspanning monomers that oligomerize to permeabilize membranes during apoptosis. *EMBO J* 2005; **24**: 2096–2103.
29. Antonsson B, Montessuit S, Lauper S, Eskes R, Martinou JC. Bax oligomerization is required for channel-forming activity in liposomes and to trigger cytochrome c release from mitochondria. *Biochem J* 2000; **345** (Part 2): 271–278.
30. Nechushtan A, Smith CL, Hsu YT, Youle RJ. Conformation of the Bax C-terminus regulates subcellular location and cell death. *EMBO J* 1999; **18**: 2330–2341.
31. Hsu YT, Youle RJ. Bax in murine thymus is a soluble monomeric protein that displays differential detergent-induced conformations. *J Biol Chem* 1998; **273**: 10777–10783.
32. Zandomeni R, Weinmann R. Inhibitory effect of 5, 6-dichloro-1-beta-D-ribofuranosylbenzimidazole on a protein kinase. *J Biol Chem* 1984; **259**: 14804–14811.
33. Kau TR, Way JC, Silver PA. Nuclear transport and cancer: from mechanism to intervention. *Nat Rev Cancer* 2004; **4**: 106–117.
34. Hibi M, Lin A, Smeal T, Minden A, Karin M. Identification of an oncoprotein- and UV-responsive protein kinase that binds and potentiates the c-Jun activation domain. *Genes Dev* 1993; **7**: 2135–2148.
35. Tournier C, Hess P, Yang DD, Xu J, Turner TK, Nimnual A *et al*. Requirement of JNK for stress-induced activation of the cytochrome c-mediated death pathway. *Science* 2000; **288**: 870–874.
36. Kharbanda S, Pandey P, Jin S, Inoue S, Bharti A, Yuan ZM *et al*. Functional interaction between DNA-PK and c-Abl in response to DNA damage. *Nature* 1997; **386**: 732–735.
37. Foray N, Marot D, Randrianarison V, Venezia ND, Picard D, Perricaudet M *et al*. Constitutive association of BRCA1 and c-Abl and its ATM-dependent disruption after irradiation. *Mol Cell Biol* 2002; **22**: 4020–4032.
38. Aladjem MI, Spike BT, Rodewald LW, Hope TJ, Klemm M, Jaenisch R *et al*. ES cells do not activate p53-dependent stress responses and undergo p53-independent apoptosis in response to DNA damage. *Curr Biol* 1998; **8**: 145–155.
39. Villunger A, Michalak EM, Coultas L, Mullauer F, Bock G, Ausserlechner MJ *et al*. p53- and drug-induced apoptotic responses mediated by BH3-only proteins puma and noxa. *Science* 2003; **302**: 1036–1038.
40. Jeffers JR, Parganas E, Lee Y, Yang C, Wang J, Brennan J *et al*. Puma is an essential mediator of p53-dependent and -independent apoptotic pathways. *Cancer Cell* 2003; **4**: 321–328.
41. Mihara M, Erster S, Zaika A, Petrenko O, Chittenden T, Pancoska P *et al*. p53 has a direct apoptogenic role at the mitochondria. *Mol Cell* 2003; **11**: 577–590.
42. Chen X, Zhang J, Lee J, Lin PS, Ford JM, Zheng N *et al*. A kinase-independent function of c-Abl in promoting proteolytic destruction of damaged DNA binding proteins. *Mol Cell* 2006; **22**: 489–499.
43. Deng X, Hofmann ER, Villanueva A, Hobert O, Copodiec P, Veach DR *et al*. Caenorhabditis elegans ABL-1 antagonizes p53-mediated germline apoptosis after ionizing irradiation. *Nat Genet* 2004; **36**: 906–912.
44. Liu P, Jenkins NA, Copeland NG. A highly efficient recombineering-based method for generating conditional knockout mutations. *Genome Res* 2003; **13**: 476–484.
45. Luo J, Su F, Chen D, Shiloh A, Gu W. Deacetylation of p53 modulates its effect on cell growth and apoptosis. *Nature* 2000; **408**: 377–381.

Supplementary Information accompanies the paper on Cell Death and Differentiation website (<http://www.nature.com/cdd>)